Journal of Global Environment Engineering, Vol. 8, pp. 1- 15, 2002

MEASUREMENTS OF OPTICAL AND CHEMICAL PROPERTIES OF AEROSOLS FOR ESTIMATES OF ATMOSPHERIC TUBIDITY OVER THE EAST CHINA SEA BY SATELLITE DATA

Shuichi Hasegawa [1]
Sachio Ohta [2]
Naoto Murao [3]
Sadamu Yamagata [4]

Abstract

The optical and chemical properties of aerosols were measured on Fukue Island from 20 April to 9 May 2000 to estimate the atmospheric turbidity coefficient (aerosol optical thickness at 1μm) over the East China Sea by satellite data. The single scattering albedo was measured using an integrating nephelometer and a Particle Soot / Absorption Photometer (PSAP) which measure scattering and absorption coefficients, respectively. The single scattering albedo mostly ranged from 0.8 to 0.9. The chemical composition of fine particles was analyzed from filter samples. The concentrations of elemental carbon and SO_4^{2-} were 0.3-1.5μg m^{-3} and 2.4-7.0μg m^{-3}, respectively, and the concentration of Al and Fe was higher during yellow dust episodes. The atmospheric turbidity coefficient was estimated from Terra MODIS data as a case study, using the measured single scattering albedo, calculated phase function based on the chemical composition, and sea surface reflectance estimated from the observed radiance and measured aerosol optical properties for the same times as the satellite data. The atmospheric turbidity coefficient was less than 0.12 over the most of the East China Sea, whereas it was more than 0.12 over the coastal sea areas of the southwestern part of the Korean Peninsula. The measurement methods for satellite remote sensing of atmospheric turbidity coefficients are discussed.

KEYWORDS: *atmospheric turbidity coefficient, satellite remote sensing, single scattering albedo, sea surface reflectance*

1. Introduction

Accurate estimates of the surface temperature is an important issue related to global warming. Although global warming is due to the increase in greenhouse gases, it has recently been pointed out

1 D.Eng, Post Doctoral Fellow, National Institute for Environmental Studies, Tsukuba 305-8506, Japan
2 D.Sci., Prof., Division of Environment and Resource Eng., Graduate School of Eng., Hokkaido Univ., Sapporo 060-8628, Japan
3 D.Eng., Associate Prof., Division of Environment and Resource Eng., Graduate School of Eng., Hokkaido Univ.
4 D.Eng., Instructor, Division of Environment and Resource Eng., Graduate School of Eng., Hokkaido Univ.

that aerosols play an important role in variations in surface temperatures. Aerosols influence the global climate by scattering and absorbing solar radiation. This has been termed the direct effect of aerosols. The direct effect of aerosols depends on both the optical thickness and optical properties such as the single scattering albedo and phase function. The optical thickness is an extinction coefficient at a certain wavelength integrated with the total air column. Satellite remote sensing is a useful means for observing the global distribution of aerosol optical thickness. The single scattering albedo and phase function are required when converting the radiance observed by satellite into optical thickness. Therefore appropriate values of these parameters based on measurements are necessary for accurate estimates of the aerosol optical thickness.

At the same time, atmospheric pollution over East Asia may be worsening due to the growing industrialization and therefore it is important to monitor the aerosol optical thickness in detail by satellite. In addition, seawater pollution such as red tides and soil discharges in coastal areas can be observed by satellite. However, atmospheric correction—the process to eliminate the effects of scattering and absorption due to air molecules, trace gases, and aerosols on the radiance observed by satellite—is required to determine the pollutant concentration quantitatively.

In this study intensive measurements of the optical and chemical properties of aerosols were carried out at ground level in Fukue Island, Nagasaki Prefecture, Japan. Scattering and absorption coefficients, chemical composition, size separated number concentration, and optical thickness were measured with a short averaging period for synchronization with satellite data, and the measurement methods for ground truth is discussed. In addition, the atmospheric turbidity coefficient over the East China Sea was estimated from the radiance observed by Terra MODIS as a case study by using the measured parameters.

2. Measurements of the optical and chemical properties of aerosols

We made intensive measurements in Fukue Island (32.73°N, 128.73°E) from 20 April to 9 May 2000. The location of Fukue Island is shown in Figure 1. Fukue Island is a rural island 100km off Kyusyu with a population of 45 thousand. The measurement site was the rooftop of a building 10m above the ground at a school in a small village facing a narrow bay. The arrangement of the measurement setup, which is described in the following sections, is shown in Figure 2.

2.1 Measurements of scattering and absorption coefficients

The scattering coefficient was measured with an integrating nephelometer (Radiance Research, M903). The nominal wavelength was 0.530μm; particle-free air was used to set the instrument zero, which was obtained by passing ambient air through a Teflon filter with high collection efficiency; CO_2 was used as a span gas with a scattering coefficient of 2.14×10^{-5} m^{-1} at 20℃ and 1 atm, as recommended by Anderson and Ogren (1998) instead of CFC-12 which has been used but is now outlawed. The calibration gas was purged from a purge port that is located at the bottom of the chamber with a sampling volume of 0.44l and it was flowed long enough to ensure replacement by the calibration gas.

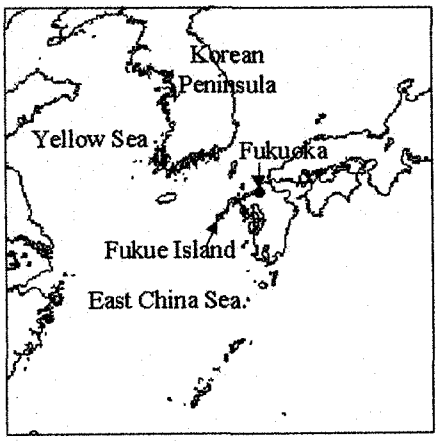

Figure 1. Location of Fukue Island.

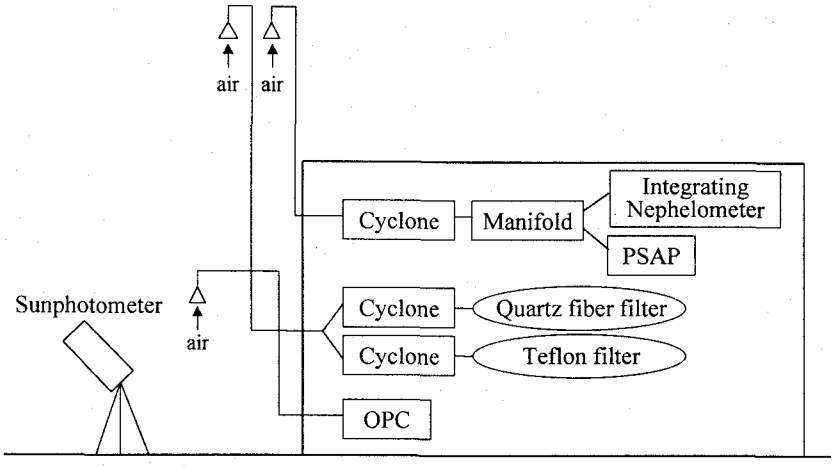

Figure 2. Schematic outline of the measurements.

The absorption coefficient was measured with a Particle Soot / Absorption Photometer (PSAP; Radiance Research). The nominal wavelength was 0.565μm. The measurement principle of PSAP is the integrating plate method with continuous sampling and measurement. The absorption coefficient s_{abs} is determined by the formula:

$$\sigma_{abs} = -\frac{A}{V}\ln T \qquad (1)$$

where A is the area of the sample spot, V is the volume of air sampled, and T is the filter transmission. The integrating plate method causes overestimation of the absorption coefficient (Horvath, 1997) by factors that cannot be eliminated; backscattering by particles including nonabsorbing particles and multiple absorption as particle loading increases. The empirical correction factor for PSAP was determined by the manufacturer with a comparison between the instrument response and the difference between extinction and scattering coefficient (Bond et al., 1999). Bond et al. (1999)

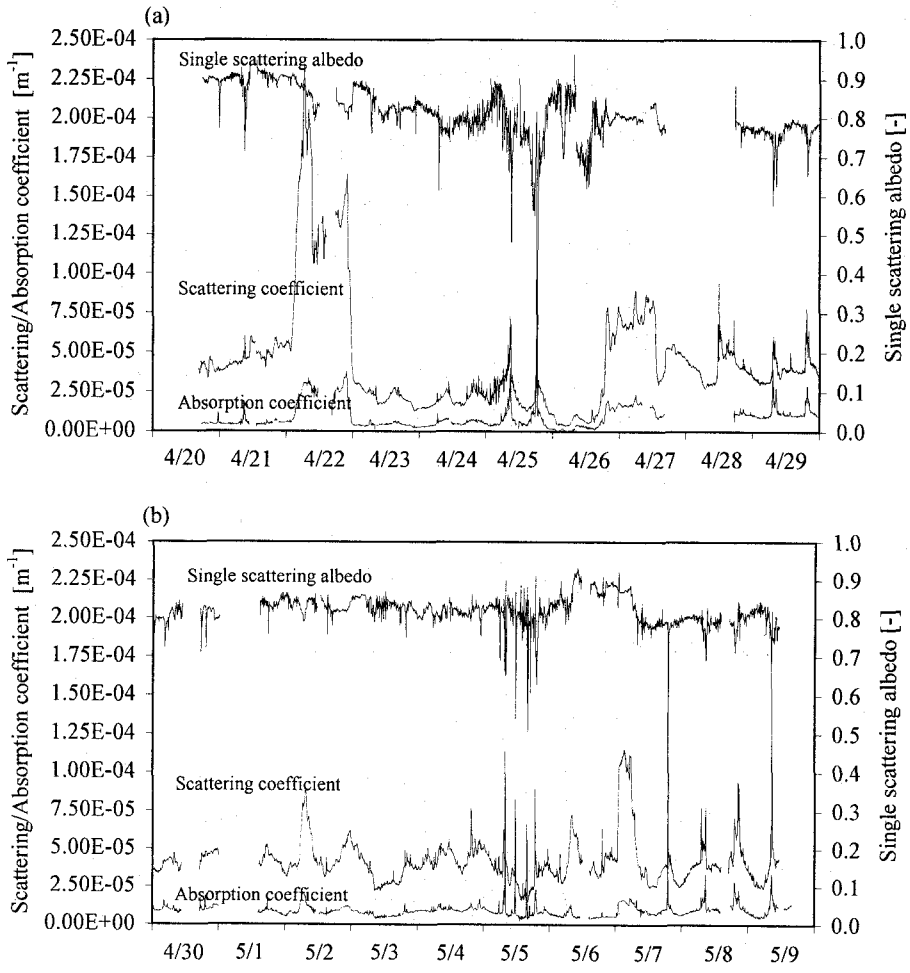

Figure 3. Scattering coefficient, absorption coefficient, and single scattering albedo in Fukue Island ; (a) from 20 to 29 April; (b) from 30 April to 9 May 2000 (JST).

investigated the dependence of the calibration on a filter transmission greater than 0.7 and found that the manufacturer's correction factor accounted for this effect satisfactorily. However, the nominal spot size on a filter was different from the actual size of PSAP used in this study. Therefore we corrected in terms of the area of the sample spot. The flow rate was measured by an internal mass flow meter (Honeywell, AWM5101; at 0℃, 1atm). The flow rate was also measured by another mass flow meter (STEC, SEF-51; at 25℃, 1atm) and modified from the flow rate measured by the former to the one measured by the latter. When the latter indicated 1.0 l min^{-1} the former indicated 0.78 l min^{-1} and this difference was within the dependence of volume on temperature plus the measurement error of these flow meters.

Both the integrating nephelometer and PSAP were situated in a house on the roof of the building. The sample air inlet was 5 m above the roof. The sample air was introduced at a flow rate of 20 l

min^{-1} to a cyclone separator with a 50% cutoff diameter of 2μm at this flow rate, followed by a manifold. The sample air was branched from the manifold to both the integrating nephelometer at 5l min^{-1} and PSAP at 1l min^{-1}, respectively. The averaging period of both instruments for each data point was 5 minutes.

Figure 3 shows the scattering coefficient, absorption coefficient, and single scattering albedo from 20 April to 9 May 2000 (JST) in Fukue Island. The scattering coefficient varied mostly between 2-6$\times 10^{-5}$ m^{-1}, whereas the absorption coefficient varied between 5-10$\times 10^{-6}$ m^{-1}, though these often increase in very short times due to refuse burning in farms and houses around the measurement site. The single scattering albedo was in the range of 0.8 to 0.9. It is noted that the Japan Meteorological Agency (2000) observed the yellow dust at the Fukue station located 11 km from the site from 5:00 on 22 April to 1:00 on 23 April and from 12:50 on 1 May to 11:30 on 2 May (JST).

2.2 Filter sampling and chemical analysis

Fine particles were sampled on quartz fiber filters (Pallflex 2500QAT-UP, 47mm) and Teflon filters (Sumitomo Fluoropore FP-1000, 47mm). The sample air inlet was 5 m above the roof and branched into two lines. Each line was connected to a cyclone separator with a 50% cutoff diameter of 2μm at 20 l min^{-1} and the fine particles were sampled on each filter.

The carbon content in the quartz fiber filter samples were determined by a combustion technique at 850°C in an NC-analyzer (Sumitomo Chemical, Sumigragh NC-80) and the analysis used a gas chromatogragh (Shimadzu, GC-14A) equipped with a Ni catalyst methanizer and flame inonization detector (FID) (Ohta and Okita, 1984). The filters were cut into quarter pieces; for each sample, one quarter was used to determine the total carbon content (TC), and another quarter was heated in an electric furnace at 300°C in ambient air for 30 minutes to remove organic carbon (OC) and then used to determine the elemental carbon content (EC). The difference between TC and EC gives the amount of OC. However, the quartz fiber filter causes a positive artifact of OC due to adsorption of organic gases (Kim et al., 2001). In this study, this artifact tended to contribute a lot to the concentration of OC when the sample volume was less than 10 m^3. Therefore the concentration of OC for this case was corrected using the ratio of the OC to EC concentration averaged by other samples whose the sample volume was more than 20 m^3. The concentrations of OC shown in Table 1 have been corrected in this way.

Half of each Teflon filter sample was used to determine the water-soluble contents. The contents were extracted ultrasonically with distilled deionized water. The concentrations of anions (SO_4^{2-}, NO_3^-, Cl^-) and cations (Na^+, NH_4^+, K^+, Ca^{2+}, Mg^{2+}) in the extracted solution were determined by an ion chromatograph (Yokogawa Analytical Systems, IC7000; column Excelpak ICS-A23 for anions and ICS-C25 for cations).

A 1/8 piece of each Teflon filter sample was used to determine the elements. This content was extracted ultrasonically in a mixed solution of nitric acid and hydrofluoric acid. The concentration of elements in the solution was determined by an inductively coupled plasma mass spectrometer (ICP-MS; Yokogawa Analytical Systems, HP4500).

Table 1 shows the sampling periods, sample volumes, and concentrations of carbon and water-

Table 1. Sampling period, sample volume, and soncentrations of carbon and water-soluble contents, and other elements of each sample.

Sample No.	Begin date (JST)	End date (JST)	Sample volume [m^3]		Concentration [$\mu g\ m^{-3}$] *1									
			Quartz	Teflon	EC	OC	Cl^-	NO_3^-	SO_4^{2-}	Na^+	NH_4^+	K^+	Ca^+	Mg^{2+}
1	4/23 8:30	4/24 11:06	31	33	0.84	2.12	0.12	0.28	2.63	0.29	0.76	0.22	0.17	0.09
2	4/24 11:18	4/25 10:28	28	29	1.34	2.98	0.00	0.10	2.79	0.05	0.97	0.24	0.09	0.04
3	4/25 10:50	4/27 10:31	56	59	0.77	2.19	0.00	0.15	3.97	0.17	1.13	0.23	0.12	0.08
4	4/27 11:08	4/28 10:40	28	29	1.29	3.65	0.02	0.31	3.83	0.34	1.16	0.34	0.11	0.13
5	4/28 10:50	4/29 10:05	27	29	1.54	3.45	0.00	0.07	4.57	0.07	1.57	0.32	0.08	0.11
6	4/29 10:16	4/29 17:30	8.7	9.1	1.24	3.60	ND	0.04	4.56	0.04	1.68	0.26	0.14	0.12
7	4/29 17:40	5/1 10:35	49	51	0.97	2.24	0.00	0.01	5.43	0.03	1.72	0.16	0.07	0.06
8	5/1 10:44	5/2 11:08	28	30	1.10	2.21	0.00	0.10	4.82	0.10	1.55	0.18	0.21	0.08
9	5/2 11:08	5/3 13:48	32	34	0.76	2.46	ND	0.04	4.13	0.12	1.41	0.15	0.10	0.07
10	5/3 13:55	5/4 10:24	24	26	0.86	2.89	0.00	0.03	3.83	0.05	1.41	0.10	0.07	0.05
11	5/4 10:33	5/4 17:26	8.3	8.6	0.95	2.75	ND	0.02	3.96	0.02	1.51	0.14	0.12	0.10
12	5/4 17:35	5/5 10:29	20	21	0.98	3.98	0.00	0.01	3.74	0.02	1.38	0.19	0.08	0.05
13*2	5/4 10:37	5/5 15:15	4.2	4.4	0.34	1.00	ND	0.01	2.35	ND	0.83	ND	ND	ND
14	5/6 15:24	5/7 10:25	22	23	0.76	2.96	0.00	0.04	6.93	0.12	2.37	0.20	0.17	0.07
15	5/7 10:32	5/7 17:21	8.1	8.5	0.97	2.81	ND	0.05	2.47	0.05	0.95	0.06	0.14	0.08
16	5/7 17:28	5/8 10:30	20	21	1.45	4.31	0.00	0.05	3.36	0.03	1.24	0.23	0.07	0.04
17	5/8 10:37	5/8 17:21	8.1	8.5	1.30	3.76	ND	0.11	4.13	0.03	1.55	0.22	0.15	0.11
18	5/8 17:27	5/9 14:27	25	26	1.56	4.46	0.00	0.08	3.99	0.03	1.36	0.39	0.07	0.04

Sample No.	Concentration [$\mu g\ m^{-3}$] *1										
	Al	V	Cr	Mn	Fe	Ni	Cu	Zn	As	Cd	Pb
1	0.165	0.001	0.001	0.006	0.126	0.001	0.006	0.023	0.002	0.000	0.021
2	0.119	0.002	ND	0.005	0.076	0.001	0.006	0.023	0.002	0.000	0.024
3	0.391	0.002	0.001	0.010	0.243	0.001	0.004	0.026	0.004	0.001	0.023
4	0.065	0.002	0.001	0.009	0.089	0.001	0.006	0.048	0.007	0.003	0.050
5	0.000	0.002	0.001	0.006	0.063	0.001	0.005	0.038	0.005	0.002	0.028
6	0.000	0.003	ND	0.003	0.032	0.001	0.007	ND	0.004	0.001	0.023
7	0.089	0.003	ND	0.004	0.083	0.001	0.003	0.017	0.002	0.001	0.012
8	0.554	0.005	0.001	0.011	0.326	0.002	0.005	0.021	0.002	0.000	0.016
9	0.119	0.002	ND	0.004	0.080	0.001	0.004	0.015	0.003	0.000	0.014
10	0.000	0.005	ND	0.002	0.032	0.002	0.004	0.009	0.003	0.000	0.010
11	0.000	0.004	ND	0.000	ND	0.002	ND	ND	0.003	0.000	0.013
12	0.074	0.003	ND	0.002	0.063	0.001	0.005	0.014	0.003	0.000	0.012
13	0.000	0.002	ND	0.000	ND	0.002	0.009	ND	0.003	ND	0.009
14	0.095	0.004	ND	0.003	0.081	0.002	0.003	0.019	0.007	0.000	0.016
15	0.000	0.003	ND	0.004	ND	0.002	ND	0.025	0.005	0.000	0.011
16	0.000	0.002	ND	0.003	0.042	0.001	0.002	0.022	0.003	0.000	0.017
17	0.000	0.002	ND	0.005	ND	0.001	ND	0.029	0.002	0.001	0.025
18	0.060	0.003	ND	0.005	0.045	0.001	0.002	0.025	0.002	0.001	0.029

*1 ND indicates the concentration lower than detection limit.
*2 The sampling was stopped for 67 minutes during the period.

soluble contents, and other elements. The concentration of EC, OC, SO_4^{2-}, and NH_4^+ were 0.3-1.5μg m^{-3}, 1.0-4.5μg m^{-3}, 2.4-7.0μg m^{-3}, and 0.8-2.4μg m^{-3} respectively. The fraction of nss- SO_4^{2-} in SO_4^{2-} was more than 0.97. The concentration of Al and Fe for samples No. 3 and No.8 were higher than the other samples due to the yellow dust. The Japan Meteorological Agency (2000) observed the yellow dust at Fukue station as mentioned in section 2.2. The typical elements of anthropogenic emissions such as V, As, Ni, and Pb did not vary among the samples.

2.3 Number concentration of size separated particles

The number concentration of particles was measured with an optical particle counter (OPC; RION, KC-01C) to monitor the yellow dust episodes and local pollution like refuse burning. The particle sizes were separated into 5 ranges: more than 0.3μm, 0.5μm, 1.0μm, 2.0μm, and 5.0μm in diameter. The OPC was situated in the house and the sample air inlet was 2 m above the roof. The sample air was introduced at 0.51 min^{-1}.

Figure 4 shows the number concentrations of each size range from 20 April to 9 May 2000 (JST). They often increase suddenly due to refuse burning around the site as mentioned in section 2.1. The increase in coarse particles (2μm<, 5μm<) from 1 May to 2 May suggested the yellow dust episode, which corresponded the observations at Fukue station by the Japan Meteorological Agency. The increase of coarse particles was also measured from 23 April to 24 April, from 26 April to 27 April, and on 8 May.

2.4 Measurement of aerosol optical thickness

The aerosol optical thickness was measured by a sunphotometer (MS-120, Eko Instruments) with the wavelengths 0.368μm, 0.500μm, 0.675μm, and 0.778μm. The measurements were carried out manually almost every hour on clear days, and 40 sets of the measurements were obtained between 20 April and 9 May 2000 (JST). The aerosol optical thickness depends on the wavelength and is expressed by

$$\tau = \beta \lambda^{-\alpha} \qquad (2)$$

where β is the atmospheric turbidity coefficient that indicates the aerosol optical thickness at 1μm, λ is the wavelength, and a is the Ångström component which indicates the dependence of the aerosol optical thickness on the wavelength. Figure 5 shows the atmospheric turbidity coefficient and Ångström component determined by the 40 sets of measurements. The atmospheric turbidity coefficient ranged from 0.08 to 0.5, and the Ångström component ranged from 0.3-1.5. On 22, 23, and 24 April the Ångström component was small (0.3-0.7) due to the high concentration of coarse particles as indicated in Figure 4.

2.5 Effect of the contribution of coarse particles on the single scattering albedo

In this study the scattering and absorption coefficients of fine particles were measured with some

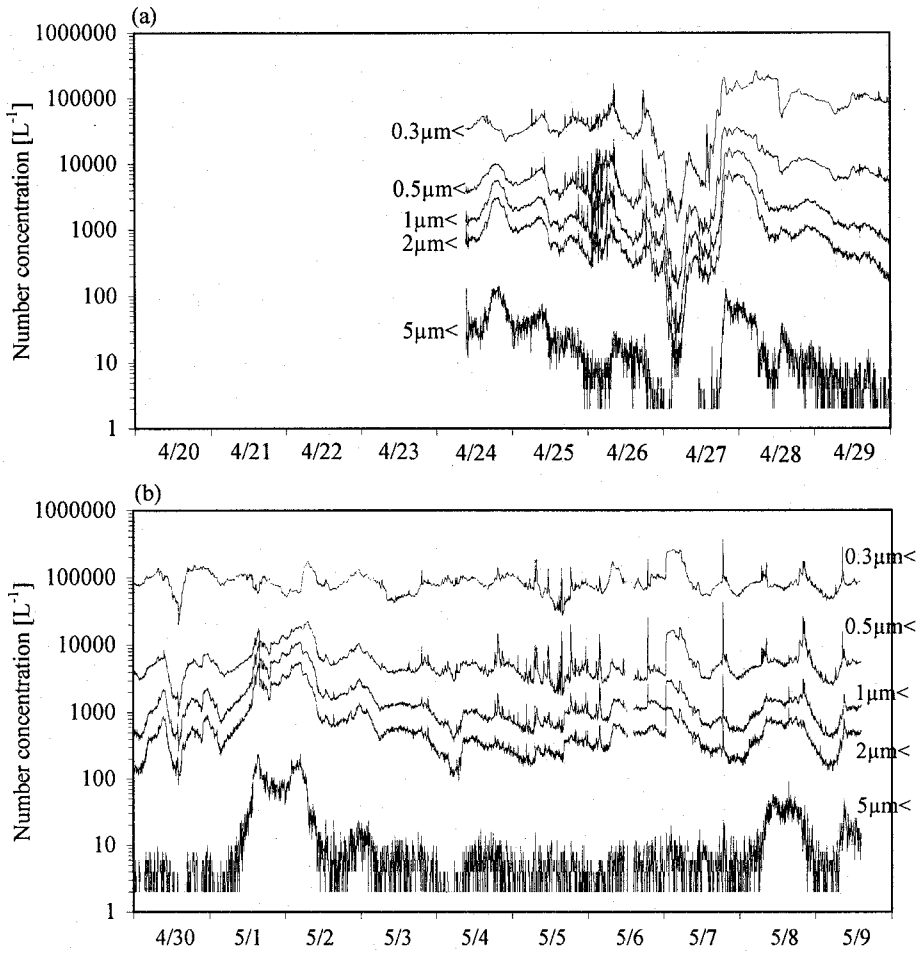

Figure 4. Number concentration of particles larger than 0.3μm, 0.5μm, 1.0μm, 2.0μm, and 5.0μm in Fukue Island; (a) from 20 to 29 April; (b) from 30 April to 9 May 2000 (JST).

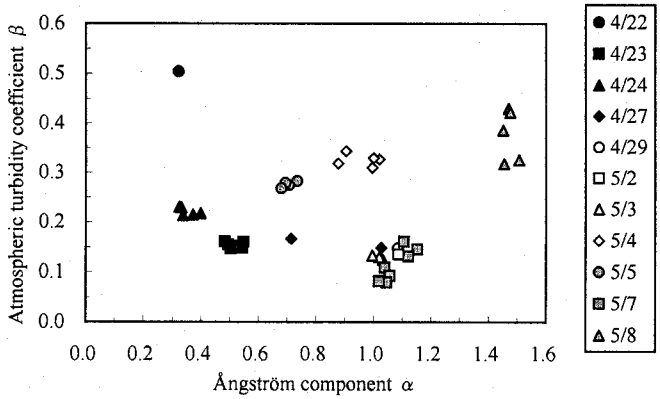

Figure 5. Relationship between the Ångström component and atmospheric turbidity coefficient measured with a sunphotometer in Fukue Island.

Table 2. Parameters used in Mie thory calculations.

Aerosol component	r_{gN}	σ_g	m_r	m_i	ρ	α
Elemental carbon	0.046	1.70	1.75	0.55	1.00	1.00
Organic compounds	0.046	1.70	1.40	0	1.40	1.00
Ammonium sulfate	0.046	1.70	1.40	2.03×10^{-9}	1.77	1.43
Ammonium nitrate	0.046	1.70	1.40	2.03×10^{-9}	1.66	1.39
Sea salt	0.490	2.15	1.40	2.03×10^{-9}	2.16	1.89
Soil	0.490	2.15	1.55	0.008	2.00	1.00

r_{gN} = Geometric number mean radius [μm]
σ_g = Geometric standard deviation
m_r = Real part of complex refractive index at 0.530 μm
m_i = Imagenary part of complex refractive index at 0.530 μm
ρ = density [g cm^{-3}]
α = growth factor with relative humidity at 75%

Table 3. Calculated single scattering albedo of fine particles only and fine plus coarse particles.

Sample No.	Single scattering albedo		Ratio*
	Fine particles	Fine and coarse particles	
1	0.831	0.871	1.05
2	0.741	0.760	1.02
3	0.858	0.855	1.00
4	0.818	0.868	1.06
5	0.772	0.790	1.02
6	0.801	0.812	1.01
7	0.840	0.840	1.00
8	0.830	0.820	0.99
9	0.854	0.865	1.01
10	0.827	0.842	1.02
11	0.811	0.817	1.01
12	0.815	0.815	1.00
13	0.860	0.860	1.00
14	0.895	0.898	1.00
15	0.768	0.791	1.03
16	0.752	0.763	1.01
17	0.786	0.795	1.01
18	0.764	0.771	1.01

* Ratio of single scattering albedo of fine and coarse particles to that of fine particles.

limitations: 1) the extinction (scattering plus absorption) of coarse particles is at most one tenth of the fine particles at normal conditions; 2) it was difficult to set the instruments outside to avoid the sampling loss of coarse particles due to maintenance of the instruments.

However, the contribution of coarse particles must be considered when the number concentration of coarse particles measured by OPC is relatively high. The single scattering albedo at 0.530μm with and without coarse particles were estimated by Mie theory calculations using the chemical composition of 18 samples obtained in this study and the parameters are shown in Table 2. It was assumed that aerosols consisted of six components: elemental carbon, organic compounds, ammonium sulfate, ammonium nitrate, sea salt, and soil. The amount of organic compounds was obtained by multiplying the amount of OC by 1.2 (Countess et al., 1980). The amount of sea salt and

soil were determined from the abundance of Na^+ in seawater, 30.6%, and Al in soil, 8.13% (Mason, 1970). A log normal size distribution was assumed, and the number geometric mean radius and geometric standard deviation are shown in Table 2. The size distribution of elemental carbon, organic compounds, ammonium sulfate, and ammonium nitrate were assumed as the fine mode. The size distribution of sea salt and soil were assumed as the coarse mode. The single scattering albedo with coarse particles was calculated assuming that analyzed concentrations of sea salt and soil was a part of the coarse mode (less than 2μm), and the total mass concentrations of sea salt and soil were extrapolated from a given mass size distribution of the coarse mode. Table 2 also shows the complex refractive index, density, and growth factor of each aerosol component. The growth factor with a relative humidity of 75% of hygroscopic components such as ammonium sulfate, ammonium nitrate, and sea salt (Tang et al., 1977, Tang, 1980) were considered.

The single scattering albedo with and without coarse particles are shown in Table 3. The differences were within 1% when the mass concentration of soil was high (i.e. yellow dust episode), because soil not only scatter but also absorb even weakly the solar radiation. However, when the mass concentration of sea salt alone was high, the single scattering albedo with coarse particles was 5-6% higher than that without coarse particles since sea salt is not the absorbent.

3. Estimate of atmospheric turbidity coefficients by satellite data

3.1 Methods

The spatial distribution of atmospheric turbidity coefficients over the East China Sea was estimated from satellite data as a case study. This study used the 1 km Calibrated Radiances Level 1B product of the Moderate-resolution Imaging Spectroradiometer (MODIS) aboard the Terra satellite. During the measurements only one case was suitable for the estimates; it was at 11:20-11:25 on 3 May 2000 (JST).

The flowchart of the calculations of the atmospheric turbidity coefficient for one image unit is shown in Figure 6. The radiative transfer calculation was carried out using solar zenith, solar azimuth, sensor zenith, and sensor azimuth at each image unit included in the product. The single scattering albedo, phase function, and sea surface reflectance shown in Table 4 were assumed to be spatially constant within the object area. For the single scattering albedo at 0.530μm the measured scattering and absorption coefficient at the same time as the satellite data was recorded were used. The phase function at 0.530μm was calculated by Mie theory based on the chemical composition analysis and the parameters shown in Table 2. The chemical composition of sample No.10 was used though sample No.9 should have been used in terms of sampling period. Sample No.9 included the end of the yellow dust episode since the fraction of crustal origin in the aerosols was relatively high. Assuming that all amounts of Al in aerosols originate from soil, the fraction of crustal origin in aerosols e is defined by

$$\varepsilon = \left(\frac{M_{Soil}}{Al_{Soil}}\right) \Big/ \left(\frac{M_{Aerosol}}{Al_{Aerosol}}\right) \qquad (3)$$

where M_{Soil} and Al_{Soil} is the abundance of an element and Al in soil, respectively, and $M_{Aerosol}$ and

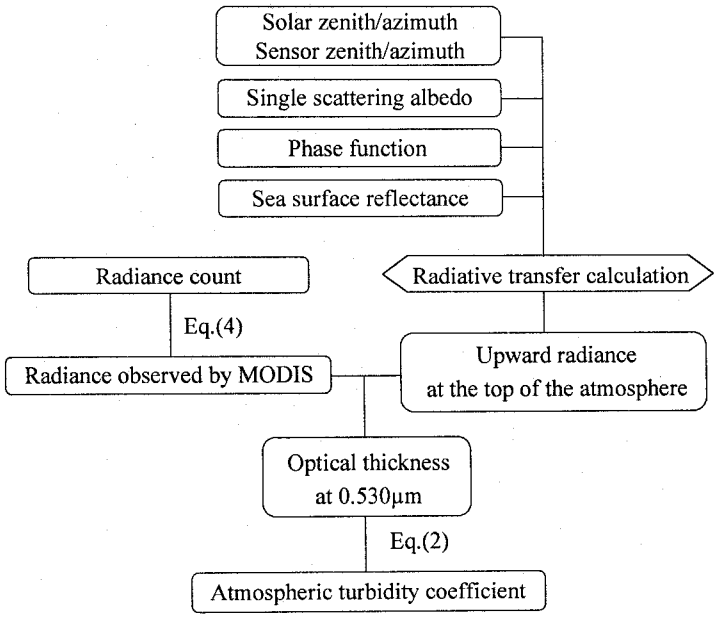

Figure 6. Flowchart of calculations of the atmospheric turbidity coefficient.

Table 4. Parameters used in the estimate of the atmospheric turbidity coefficient.

Scattering coefficient [m^{-1}]	4.26×10^{-6}
Absorption coefficient [m^{-1}]	2.56×10^{-5}
Single scattering albedo	0.857
Sea surface reflectance	0.0211
Ångström component	1.03

$Al_{Aerosol}$ are the concentrations of the element and Al in the aerosols. The composition of soil (Kitano and Matsuno, 1980) was assumed. The fraction for Ca, which is a typical element in the yellow dust, was 0.7 for sample No.9, and was in the same level as in sample No.8. It is noted that the concentrations of carbon and water-soluble content for sample No.10 were very similar to sample No.9.

The sea surface is assumed to be a Lambert surface and its reflectance was determined from the radiative transfer calculation using the radiance on the sea a few kilometers away from the measurement site, the measured single scattering albedo, the phase function calculated in the way mentioned above, and the aerosol optical thickness measured with the sunphotometer almost at the same time as the satellite data was recorded.

Band 11 (0.526-0.536μm) was selected for the estimate of atmospheric turbidity coefficients. A radiance count C of band 11 was converted to a radiance I by

$$I = Scale\ (C - Offset) \quad (4)$$

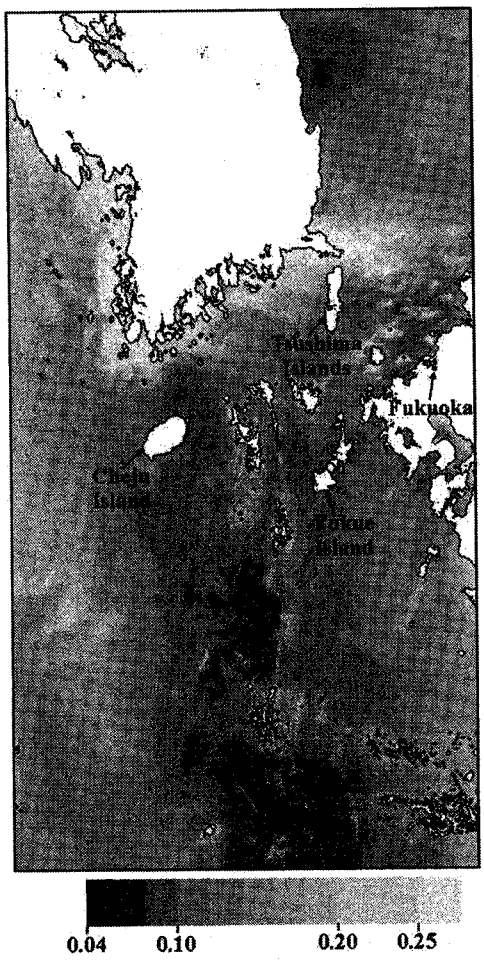

Figure 7. Image of the atmospheric turbidity coefficient over the East China Sea at 11:20-11:25 on 3 May 2000 (JST). Note that the white parts in the image are land or clouds.

where *Scale* and *Offset* were given in the product. The optical thickness at 0.530μm was determined when the upward radiance at the top of the atmosphere obtained by the radiative transfer calculation corresponded to the radiance observed by MODIS. The discrete ordinate method (Stamnes et al., 1988) was used for the radiative transfer calculation. The atmosphere was assumed to have one layer for simplicity. The land and clouds were distinguished using band 16 (0.862-0.877μm). When a radiance count of an image unit of band 16 was saturated, the unit was determined as land or clouds. The optical thickness at 0.530μm was converted into the atmospheric turbidity coefficient by equation (2). The Ångström component measured over Fukue Island with the sunphotometer almost at the same time as the satellite data was assumed to be constant spatially within the object area.

3.2 Results

Figure 7 shows an image of the atmospheric turbidity coefficient over the East China Sea at 11:20-11:25 on 3 May 2000 (JST). Note that the white parts in the image are land or clouds. The

turbidity coefficient over most of the East China Sea was less than 0.12 and decreased with distance from land. However, the turbidity coefficient over the coastal sea at the southwestern part of the Korean Peninsula was higher than that off the coast and was more than 0.20. The high values around the coastal sea of the southeastern part of the Korean Peninsula and the Tsushima Islands seemed to be affected by thin clouds that could not be eliminated completely, as was also suggested by the image of band 31 (10.78-11.28μm). The turbidity coefficient ranged from 0.12 to 0.20 on the southwestern sea of Cheju Island. The turbidity coefficient obtained from the observation of direct solar radiation (Yamamoto et al., 1968) in Fukuoka at 11:34 on 3 May 2000 (JST) was 0.18, whereas it was around 0.16-0.20 at sea a few kilometers from Fukuoka (Hakata Bay) in Figure 7.

4. Discussion

The integrating nephelometer and PSAP have the advantage of measuring the single scattering albedo for the ground truth of satellite data since these instruments measure the scattering and absorption directly, and the outputs can be obtained immediately. The single scattering albedo at the same time as a satellite observes an area including the measurement site can be used for radiative transfer calculations with high time resolution of measurements. The OPC, which is able to measure the number concentration of both fine and coarse particles, is useful to monitor an increase in coarse particles and local pollution like refuse burning. In this study the aerosol optical thickness was measured by the manually operated sunphotometer. If an automatically operated sunphotometer is available, the routine measurements for ground truth of satellite data can be composed by the integrating nephelometer, PSAP, OPC, and sunphotometer, and it is possible to carry out the measurements at different places. However, the phase function must be assumed by, for example, Mie theory calculations based on the averaged chemical composition as adopted in this study.

The sea surface reflectance was 2.1% in the case of Figure 7, and it was determined from the radiative transfer calculation using the observed radiance on the sea a few kilometers from the measurement site. This value of the sea surface reflectance is in the range of an unpolluted sea. However, it may differ due to, for example, eutrophication or soil discharge from rivers. If the concentration of chlorophyll increases, the sea surface reflectance at 0.530μm becomes smaller than over clear sea areas (Kobayashi, 1999), which means that the turbidity coefficient is generally higher even though the radiance is the same. When the concentration of yellow soil in the sea increases, the sea surface reflectance at 0.530μm becomes larger than over clear sea areas (Kobayashi, 1999), which means that the turbidity coefficient is generally smaller for the same radiance. Therefore it is also important to determine the sea surface reflectance by direct measurements at several points of the sea with a spectroradiometer.

5. Summary

The optical and chemical properties of aerosols were measured in Fukue Island from 20 April to 9 May 2000 to estimate the atmospheric turbidity coefficient over the East China Sea by satellite data. The single scattering albedo was measured using an integrating nephelometer and a Particle Soot / Absorption Photometer (PSAP) every 5 minutes. The single scattering albedo mostly ranged from 0.8

to 0.9. The chemical composition of fine particles was analyzed from 18 filter samples. The concentrations of elemental carbon and SO_4^{2-} were 0.3-1.5μg m^{-3} and 2.4-7.0μg m^{-3}, respectively, and the concentration of Al and Fe was higher during yellow dust episodes.

The atmospheric turbidity coefficient at 11:20-11:25 on 3 May 2000 (JST) was estimated from Terra MODIS data as a case study, using the measured single scattering albedo, calculated phase function based on the chemical composition, and sea surface reflectance estimated from the observed radiance and measured optical properties of aerosols at the same time as the satellite data was recorded. The atmospheric turbidity coefficient was less than 0.12 over most of the East China Sea, whereas it was more than 0.12 over the coastal sea areas of the southwestern part of the Korean Peninsula. The turbidity coefficient obtained from the direct solar radiation measurements in Fukuoka was 0.18, whereas it was around 0.16-0.20 on the sea a few kilometers from Fukuoka.

The measurement methods for satellite remote sensing of atmospheric turbidity coefficients are discussed. We conclude that routine measurements can be composed by the integrating nephelometer, PSAP, OPC, and sunphotometer. However, the phase function must be assumed by, for example, Mie theory calculations based on the averaged chemical composition. It is also important to determine the sea surface reflectance by direct measurements at points over the sea with a spectroradiometer, since it may vary due to, for example, eutrophication or soil discharge from rivers.

Acknowledgements

The Terra MODIS data was provided by the Goddard Earth Sciences Distributed Active Archive Center (GES DAAC), NASA, and the data is the property of the government of the United States of America.

References

Anderson, T. L. and Ogren, J. A. (1998) : Determining aerosol radiative properties using the TSI 3563 integrating nephelometer, Aerosol Science and Technology, Vol.29, pp57-69.

Bond, T. C., Campbell, T. L. and Anderson, D. (1999) : Calibration and intercomparison of filter-based measurements of visible light absorption by aerosols, Aerosol Science and Technology, Vol.30, pp582-600.

Countess, R.J., Wolff, G.T. and Cadle, S.H. (1980) : The Denver winter aerosol: A comprehensive chemical characterization, Journal of the Air Pollution Control Association, Vol.30, No.11, pp1194-1200.

Horvath, H. (1997) : Experimental calibration for aerosol light absorption measurements using the integrating plate method-summary of the data, Journal of Aerosol Science, Vol.28, No.7, pp1149-1161.

Japan Meteorological Agency (2000) : Surface meteorological observation report, Japan Meteorological Agency. (in Japanese).

Kim, B.M., Cassmassi, J., Hogo, H. and Zeldin, M.D. (2001) : Positive organic carbon artifacts on filter medium during $PM_{2.5}$ sampling in the South Coast Air Basin. Aerosol Science and Technology, Vol.34, pp35-41.

Kitano, Y. and Matsuno, T. (1980) : Geochemistry and environmental chemistry, Iwanami Press, 301pp. (in Japanese).

Kobayashi, H. (1999) : Satellite remote sensing of ocean colors in polluted coastal zones, Doctoral dissertation, Hokkaido Univ., Sapporo, Japan. (in Japanese).

Mason, B. (translated by Matsui, M. and Ichikuni, M.) (1970) : Principles of geochemistry, Iwanami Press, 402pp. (in Japanese).

Ohta, S. and Okita, T. (1984) : Measurements of particulate carbon in urban and marine air in Japanese areas, Atmospheric Environment, Vol.18, No.11, pp2439-2445.

Stamnes, K., Tsay, S-C., Wiscombe, W. and Jayaweera, K. (1988) : Numerically stable algorithm for discrete-ordinate-method radiative transfer in multiple scattering and emitting layered media. Applied Optics, Vol.27, No.12, pp2502-2509.

Tang, I. N., Munkelwitz H.R., Davis and J.G. (1977) : Aerosol growth studies-Ⅱ. Preparation and growth measurement of monodisperse salt aerosols. Journal of Aerosol Science, Vol.8, pp149-159.

Tang, I. N. (1980) : Deliquescence properties and particle size change of hygroscopic aerosols, Generation of Aerosols and Faculties for Exposure Experiments. Ann Arbor Sci., Ann Arbor.

Yamamoto, G., Tanaka, M. and Arao, K. (1968) : Hemispherical distribution of turbidity coefficient as estimated from direct solar radiation measurements. Journal of Meteorological Society of Japan, Vol.46, No.4, pp287-300.